

We are IntechOpen, the world's leading publisher of Open Access books Built by scientists, for scientists

6,900

Open access books available

186,000

International authors and editors

200M

Downloads

Our authors are among the

154

Countries delivered to

TOP 1%

most cited scientists

12.2%

Contributors from top 500 universities



WEB OF SCIENCE™

Selection of our books indexed in the Book Citation Index
in Web of Science™ Core Collection (BKCI)

Interested in publishing with us?
Contact book.department@intechopen.com

Numbers displayed above are based on latest data collected.
For more information visit www.intechopen.com



Full-Color Holographic Optical Elements for Augmented Reality Display

Hui-Ying Wu, Chang-Won Shin and Nam Kim

Abstract

Holographic optical element is widely developed in augmented reality, virtual reality, and three-dimensional display application. Especially, the full-color HOE has been studied for the wearable device in these days. In this chapter, the basic theories and the specific analysis for the full-color holographic optical element are explained. It also explores the Bragg angle shift phenomenon caused by shrinkage of the recording materials. The full-color holographic optical element with enhanced diffraction efficiencies using the optimum recording intensities for each wavelength is presented. The fabricated full-color holographic optical element can be applied in augmented reality application. In addition, we reviewed the waveguide head-mounted display system using full-color holographic optical element.

Keywords: holographic optical element (HOE), diffraction efficiency, augmented reality (AR), photopolymer

1. Introduction

The development of display technology, which combines electronic components and fine-patterning technology, is leading to the development of advanced augmented reality (AR)/virtual reality (VR) display devices that can realize the three-dimensional (3D) world. VR is that users can use electronic equipment such as helmets to see information about a computer-generated virtual environment. And AR is a technology that integrates graphics from the computer screen or mobile display into real-world environments. In other words, AR is one of the forms in which VR is combined with reality. Head-mounted display (HMD) has been widely used in VR and AR applications [1–4]. HMD is an imaging device that can be worn on the head like a pair of glasses or a helmet [5]. Typical AR products include Microsoft's HoloLens, Google Glass and Sony's Smart Glass, while VR products include Oculus Rift, HTC Vive Pro and Samsung Gear. The basic components applicable to these AR and VR devices can be divided into electronic components and optical components. The main parts of the optical components are the diffractive optical element (DOE) [6, 7] and the holographic optical element (HOE) [8, 9]. Because DOE uses dry etching to produce fine patterns, the process is more complex than HOE production using the holographic record methods, and the costs of production are higher. While the HOE can control the angles of the two recording beams to record the interference pattern of the beams on the recording materials, so it can be produced more simply than DOE production.

The HOE is the latest area of application of holography, where a lot of interest and research is being conducted, and many conventional optical elements (such as a lens, filter, or diffraction grating) are now being replaced by the HOE [10–15]. A HOE is an optical element designed to reproduce or deform wavefront recorded on a hologram to obtain the desired wavefront. The HOE is applied in many fields because they are mass-produced, cheap, and can perform multiple functions simultaneously with a single element. Recently, it has begun to be applied to holographic head up display (HUD) systems, head-mounted display (HMD) that show driving information in front of the driver’s eyes without looking at the dashboard of the car [16]. In 2015, Sony released the transparent lens eyewear “SmartEyeGlass Developer Edition”. It includes a CMOS image sensor, accelerometer, gyroscope, electronic compass, brightness sensor, and microphone. Also, it is equipped with holographic waveguide technology to achieve high transparency of 85% and a thin, lightweight display.

In this chapter, the waveguide HMD system using full-color HOE is reviewed. And then it explores the Bragg angle shift phenomenon caused by shrinkage of the recording materials. The full-color HOE with enhanced diffraction efficiencies using the optimum recording intensities for each wavelength will be presented. The fabricated full-color HOE can be applied in the AR application.

2. Full-color HOE for waveguide-type HMD

When the HOE is applied to the HMD system, it can reduce the size of the overall device and the system becomes considerably lighter than the conventional HMD systems. Holographic waveguide HMD based on HOE is widely studied and developed in AR application.

Piao et al. proposed a full-color HOE using a photopolymer for a waveguide-type HMD [17]. **Figure 1** shows the schematic configuration of a holographic waveguide HMD. The waveguide HMD system can be simplified by replacing the mirror or lens of the system with HOE. The first HOE diffracts the magnified image from micro-display and the diffracted image is guided inside the waveguide plate with the total internal reflection. Finally, the guided light diffracted by the second HOE projects the image to the observers.

In order to provide the full-color HOE, the optical efficiencies of the full-color HOE with different structures are measured, as shown in **Figure 2**. Here, the optical efficiency is the intensity ratio of the diffracted beam to the incident beam. When the HOE is recorded by three wavelengths simultaneously in one photopolymer, the optical efficiencies for the three wavelengths were 16, 20, and 10%, respectively. And when the HOE is recorded in the three-layer structure, the optical efficiency of the most exterior layer is too low to provide the full-color image. So the two-layer

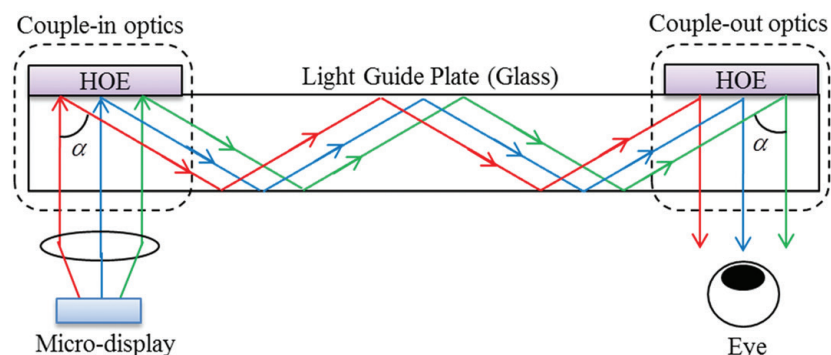


Figure 1.
The schematic configuration of a holographic waveguide HMD.

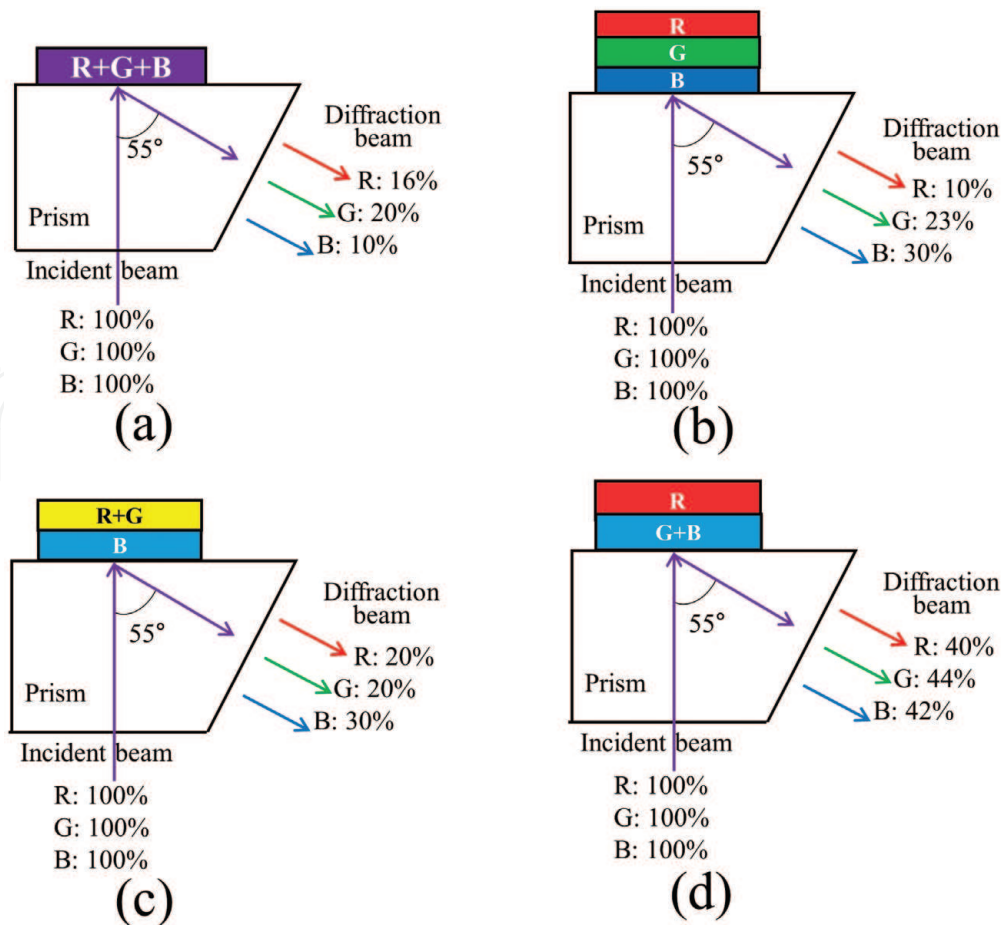
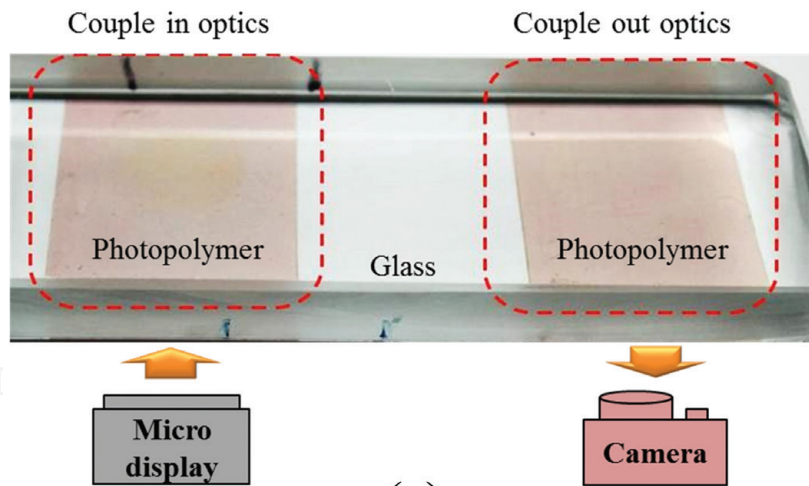


Figure 2. The efficiency of the full-color HOEs for (a) one-layer structure, (b) three-layer structure, and (c) two-layer structure (RG/B) (d) two-layer structure (R/GB).

laminated-structure is utilized to obtain higher optical efficiency. The photopolymer has different transmittance for three wavelengths. The transmittances were measured as 85% for red, 73% for green, and 70% for blue wavelength. So two kinds of laminated-structure were considered to fabricate the full-color HOE. As shown in **Figure 2(d)**, the optical efficiencies were measured 40, 44, and 42%, respectively for each wavelength. It was much higher optical efficiency than the other two-layer structure. Thus, the laminated full-color HOEs using the two-layer structure (R/GB) were applied in waveguide HMD system, as shown in **Figure 3**. The experimental results show that the fabricated full-color HOEs can be used in the waveguide HMD system to display high-quality color images.

For reducing the thickness of the glass substrate, Piao et al. designed a wedge-shaped waveguide HMD system that achieved high levels of color uniformity and optical efficiency [18]. **Figure 4** shows the schematic configuration of a designed waveguide structure. The basic principle of the designed waveguide system is similar to the conventional waveguide system. In this system, in and out-coupled optics were designed as wedge-shaped with a certain angle. And two reflection holographic volume gratings (HVGs) are attached on each side of the wedge-shaped waveguide to guide the images generated using a micro-display to the observers. As shown in **Figure 4(b)**, the incident angles of the recording material θ_1 and θ_2 determine the angle of the total internal reflection $\theta_t = \theta_1 + \theta_2$. The angle of the total internal reflection should be larger than the critical angle of the waveguide. And the slope angle of the wedge designed as $\theta_w = 30^\circ$ is the same with θ_2 . According to the analyses of the angular and spectral selectivity of the HVG [19], the incident angles $\theta_1 = 40^\circ$ and $\theta_2 = 30^\circ$ are suitable for recording the HVGs, which were attached



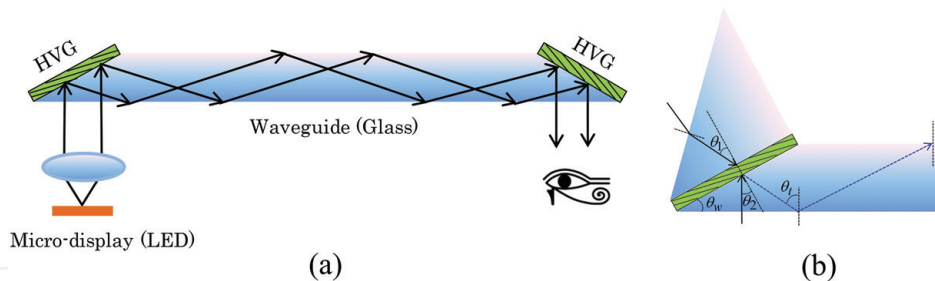
(a)



(b)

(c)

Figure 3. (a) Holographic waveguide HMD system, (b) the original image, and (c) the guided full-color image.



(a)

(b)

Figure 4. (a) The schematic configuration of a wedge-shaped holographic waveguide HMD, (b) designed angle of the light path inside the wavelength.

on both sides of the wedge-shaped waveguide. The angle of the total internal reflection is directly related to the thickness of the waveguide structure. Because of the large angle of the total internal reflection, the thickness of the designed waveguide can be reduced to 1.6 times in comparison with the conventional system.

For recording the full-color HVG in one photopolymer, a multicolor reflection HVG recording method was developed for wearable display system with good color uniformity. The diffraction efficiency was improved by controlling the exposure time of each wavelength repeatedly. **Figure 5** shows the schematic of a multicolor reflection HVG recording. Shutters were used to controlling the exposure time of each wavelength.

The optical efficiencies of the multicolor HVGs with different sequence recording processes for three wavelengths are measured, as shown in **Table 1**. The results

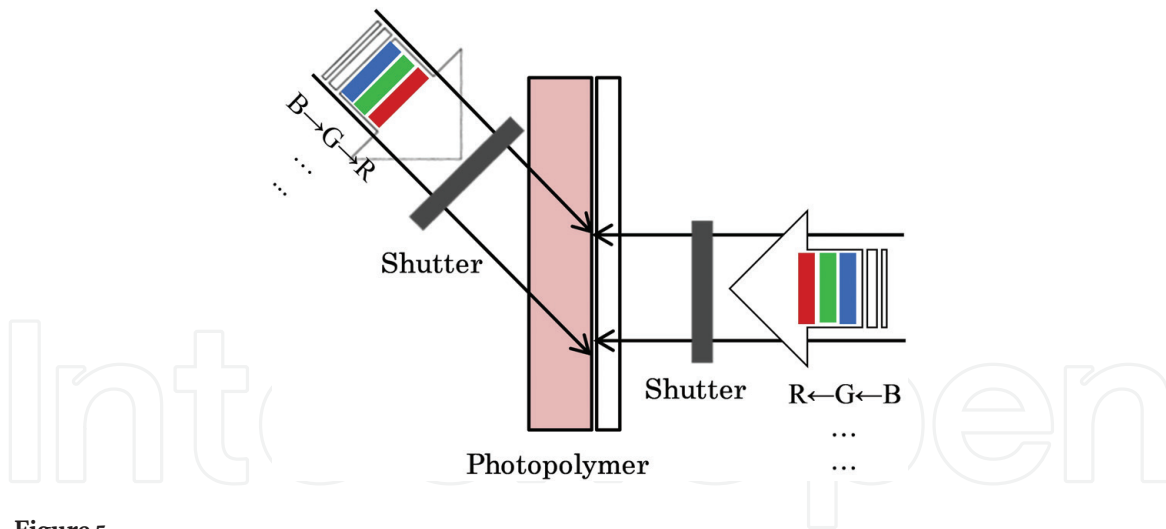


Figure 5.
 Schematic of a multicolor reflection HVG recording.

Sequence of HVGs recording	Optical efficiency for each color (%)		
R G B	R (50)	G (28.6)	B (5)
R B G	R (62)	B (46)	G (31)
G R B	G (34.4)	R (51)	B (7)
G B R	G (49)	B (47)	R (44)
B R G	B (21.6)	B (59)	G (17.8)
B G R	B (15.7)	G (37.4)	R (16.4)

Table 1.
 Optical efficiency of multicolor HVGs through different sequence recording processes.

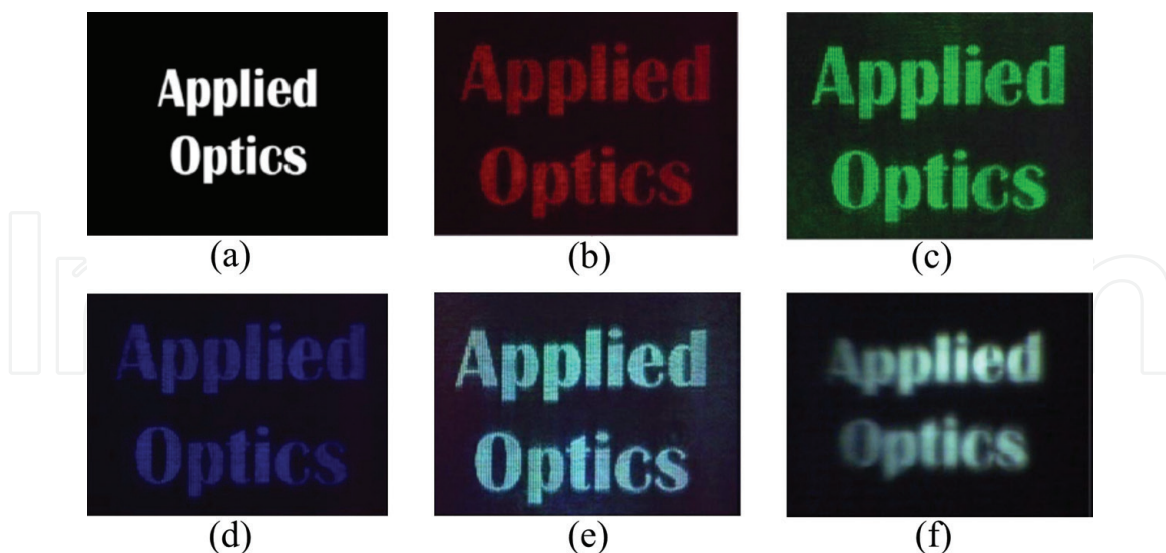


Figure 6.
 Experimental results (a) original test image, output images fabricated by (b) 633 nm, (c) 532 nm, and (d) 473 nm, and (e) the GBR sequential exposure in the SLM system, (f) the GBR sequential exposure in the micro-display system.

show that the GBR recording process exhibits much higher optical efficiency and more uniform distribution than other sequential recording processes and has a high potential for obtaining high image quality.

The fabricated HVGs recorded in one photopolymer by GBR recording process were applied to the wedge-shaped waveguide system. The output images through

the waveguide system were shown in **Figure 6**. The optical efficiencies of the monochromatic HVGs through the holographic waveguide system were measured as 30% for red, 34% for green, and 28% for blue wavelength. And the optical efficiency of the full-color HVG using the GBR recording process was measured 31%. **Figure 6(b)–(d)** show the output images through the wedge-shaped waveguide with each monochromatic HVGs attached. And **Figure 6(e)** shows the output image diffracted by the full-color HVGs recorded using the GBR recording process. The output image illuminated by a light emitting diode (LED) source was captured by the camera, as shown in **Figure 6(f)**. The image was clearly reproduced in white enough to be applicable to holographic waveguide HMD systems.

3. Full-color HOE for AR application

The full-color HOE, which has been studied in the past, is still thick and has some problems that need to be improved. In this section, the shrinkage compensation method was proposed to solve the Bragg angle shift phenomenon caused by the shrinkage of the recording materials in the holographic recording. And the iterative exposure time method is complicated in the recording process. So, the optimum recording intensities for each wavelength were experimentally investigated to record the three wavelengths at the same time. The fabricated full-color HOE achieved uniform diffraction efficiencies in the three wavelengths.

3.1 Measurement and compensation of shrinkage

In recording the hologram, the refraction index modulation occurs, and shrinkage of the recording materials occurs in the recording and UV heating process [20, 21]. The maximum diffraction efficiency is not measured at the designed recording angle because of the shrinkage of the recording materials, but at the shifted angle ($\Delta\theta_B$), it can reach the maximum diffraction efficiency [22].

An optical system has been implemented to compensate for the shrinkage of the recording materials. Through the optical system, it can measure the shifted angle from the Bragg angle, and then calculate the compensated value to record the hologram with the new recording angle.

Figure 7 shows a geometric configuration of the relationship between the reference beam and the signal beam for the shrinkage and compensation in the reflective asymmetric recording structure.

R is the reference beam with the incident angle θ_R , and S is the signal beam with the incident angle θ_S . R' and S' represent the reference beam and signal beam at the locations where the maximum diffraction efficiencies are measured due to the shrinkage of the recording materials respectively. R'' and S'' represent the reference beam and signal beam of the new calculated recording angles, considering the shrinkage compensation method. In addition, $\theta_{R'}$ is the shifted angle ($\Delta\theta_{BR}$) between the recorded reference beam R and the measured reference beam R'. $\theta_{S'}$ is the shifted angle ($\Delta\theta_{BS}$) between the recorded signal beam S and the measured signal beam S'. $\theta_{R''}$ and $\theta_{S''}$ are the calculated recording angles to compensate for the shrinkage.

The shrinkage of the recording materials is calculated by

$$d/\tan\varphi = d'/\tan\varphi' \quad (1)$$

$$Sh = (d - d')/d \times 100\% \quad (2)$$

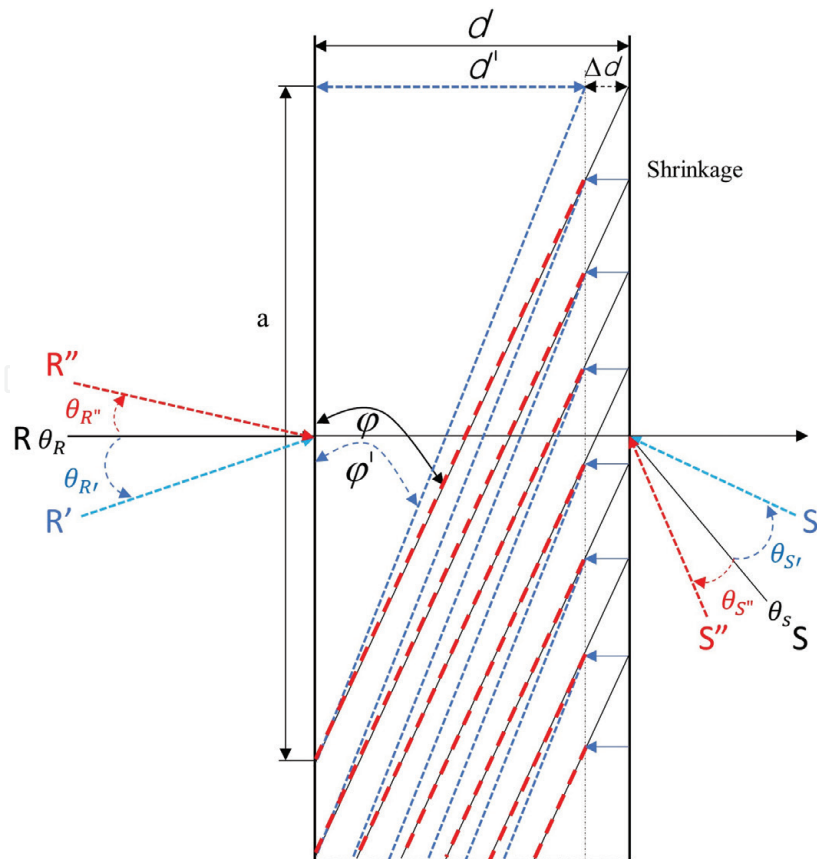


Figure 7.
 Shrinkage and compensation diagram in reflective recording structure.

where d is the thickness of the material, and d' is the thickness of the material after recording the grating. And φ is the slanted angle of the designed grating, and φ' is the slanted angle of the recorded grating.

After recording the grating, the Bragg angle is shifted to obtain the maximum diffraction efficiency. The shifted angle $\Delta\theta_B$ can be obtained by the shrinkage of the recording materials. When the new recording angles are calculated by $-1/2 \times \Delta\theta_B$, it can completely compensate the shrinkage to obtain the maximum diffraction efficiency at the designed recording angle.

3.2 Optimization of recording full-color HOE

The diffraction efficiency is the performance of the HOE, is measured using different exposure energies and different recording angles. When recording the HOE using a monochromatic wavelength, it's no need to concern about the effects of other wavelengths. However, when three wavelengths red, green and blue are exposed to record the grating at the same time, the response time of the recording materials vary depending on the absorption of the materials that react to each wavelength.

Three laser wavelengths, 633 nm (red) of JDSU company, 532 nm (green) of Cobolt company, 473 nm (blue) of Cobolt company are selected. And the recording material used in this section is a Bayfol HX102 photopolymer. The photopolymer has the fastest response in the red wavelength and the slowest response in the blue wavelength, so a full-color HOE should be recorded with different recording intensities.

Figure 8 shows an optical recording system diagram for recording full-color HOE. It shows the color of the laser beams for each wavelength and the color characteristics that can be expressed when laser beams are mixed with two wavelengths respectively. When recording the full-color HOE, the uniformity of the laser beam of three wavelengths will determine the color uniformity of full-color images.

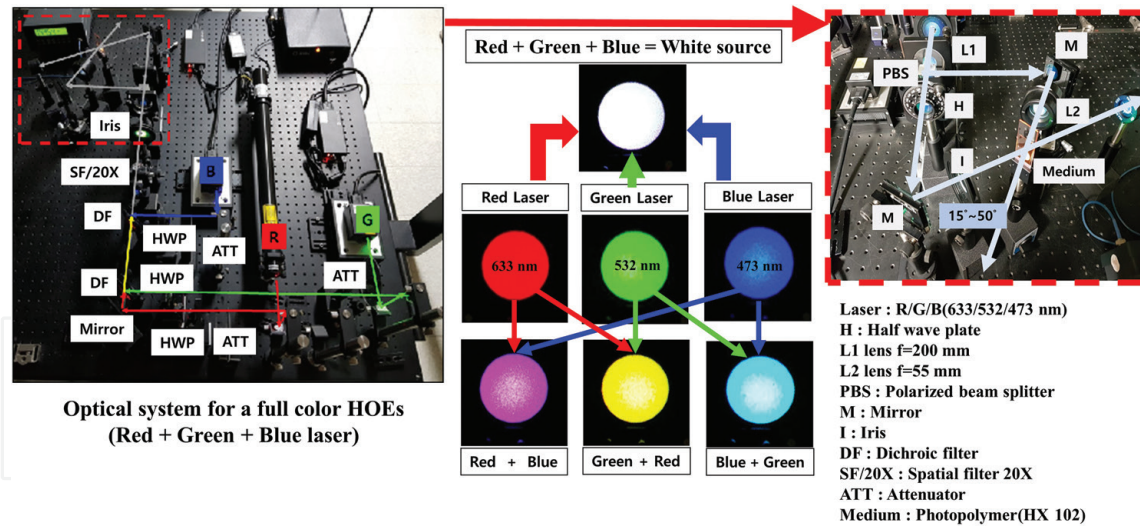


Figure 8.
Optical recording system for full-color HOE lens.

The characteristics of the photopolymer have significant effects on the many applications. Especially, the recording angles and recording intensities are very important to determine the diffraction efficiencies of the HOE. The optimized recording angle was fixed at 30° by measuring the diffraction efficiencies of different recording angles using green wavelength. Then the optical experiments were implemented corresponding to the different recording intensities for each wavelength.

If the recording intensity of each wavelength is higher than 1 mW/cm^2 when recording full-color HOE, the response time of each wavelength is so faster that the refractive index modulation reaches the saturation area quickly, causing the diffraction efficiency of each wavelength to be inconsistent or lower. And if the recording intensity is less than 0.1 mW/cm^2 , before the monomer is polymerized, the photo initiators will react first, resulting in lower diffraction efficiency. Thus, through the analysis of the inhibition period of the recording material for each wavelength and the response time, the intensity of each wavelength was applied in order of blue, green and red, which allows the three wavelengths to respond to the recording material at the same time.

Figure 9 shows the inhibition period for each wavelength is different corresponding to the recording intensity. Considering the recording intensity of each wavelength, the full-color HOE can be expressed more uniformly.

In **Table 2**, the highest diffraction efficiency was achieved when the optimized recording intensity for each wavelength was a red wavelength of 0.1 mW/cm^2 , a green wavelength of 0.11 mW/cm^2 , and a blue wavelength of 0.25 mW/cm^2 , respectively.

3.3 Full-color image for HUD with HOE lens

Figure 10 shows the experimental configuration for HUD using monochromatic grating. The focal length of the collimating lens is 25 mm.

To compare the image distortion that occurs during HUD implementation using HOE, a monochromatic display (green) with a size of $6 \text{ mm} \times 3 \text{ mm}$ and the brightness of 1000 cd/m^2 was used. **Figure 11** shows reconstruction images of the monochromatic grating at asymmetric recording angles and symmetric recording angles. The results of the reconstruction images show that the greater the recording angle, the more severe the image distortion caused by astigmatism. The reconstruction images of the grating recorded at the symmetric structure are better than the

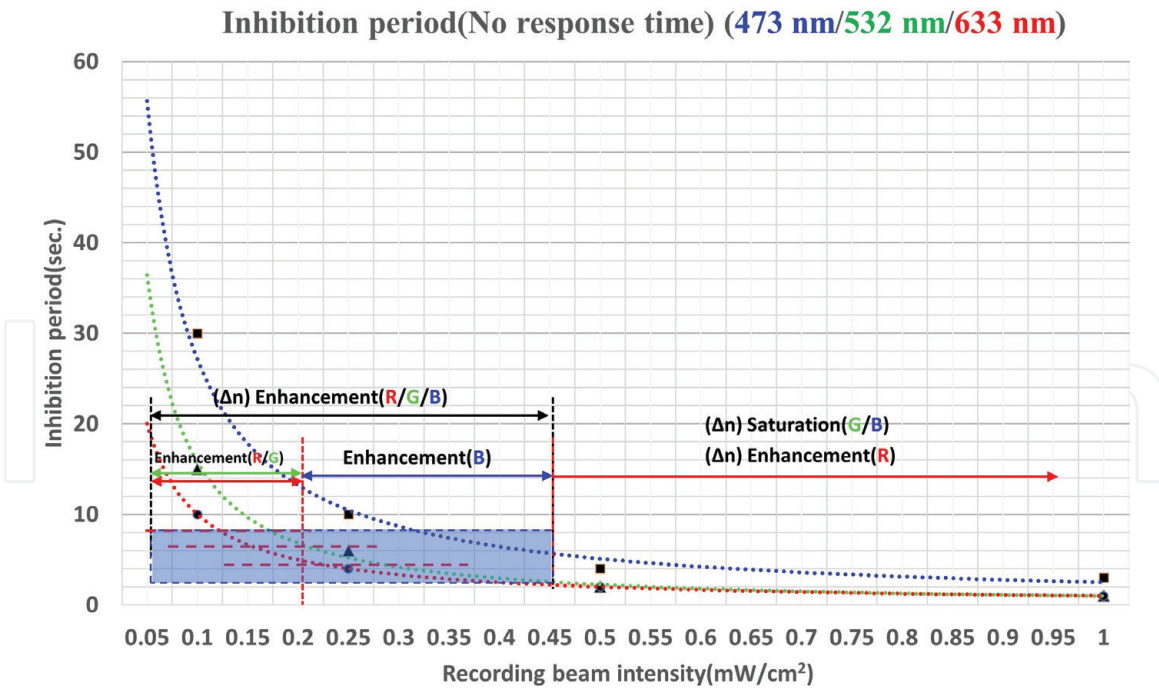


Figure 9.
 Inhibition period according to each wavelength.

633 nm (mW/cm ²)	532 nm (mW/cm ²)	473 nm (mW/cm ²)	Average D. E. (%)
1	1	2.5	42.3
0.5	0.5	1	50.5
0.2	0.25	0.45	54.1
0.1	0.125	0.25	54.5
0.1	0.11	0.25	56.84
0.075	0.0825	0.1875	50.4
0.05	0.055	0.125	47.0
0.01	0.011	0.025	5.01

Table 2.
 Diffraction efficiency according to recording intensities for each wavelength.

asymmetric structure. In the holographic recording, when the grating is recorded in symmetric structure with small recording angle, it can minimize the effect of astigmatism. But the diffraction efficiency of the recording material depends on the recording angle, it is important to select the optimum recording angle considering the diffraction efficiency.

Figure 12 shows a micro display spectrum compares with wavelength selectivity of red, green and blue. Because the spectral bandwidth of micro display used as HUD display differs from the wavelength selectivity bandwidth of the diffraction grating, the reflection images and diffraction images were analyzed to have large differences of color in order of red, green and blue.

Although there is a color difference, the full-color HOE can be used to express the color sufficiently, as shown in **Figure 13**. However, because the wavelength selectivity bandwidth of the recording materials is narrower than the spectral bandwidth of micro display, the visible brightness corresponds to the wavelength selectivity of the recording materials. When the spectral bandwidth of micro display

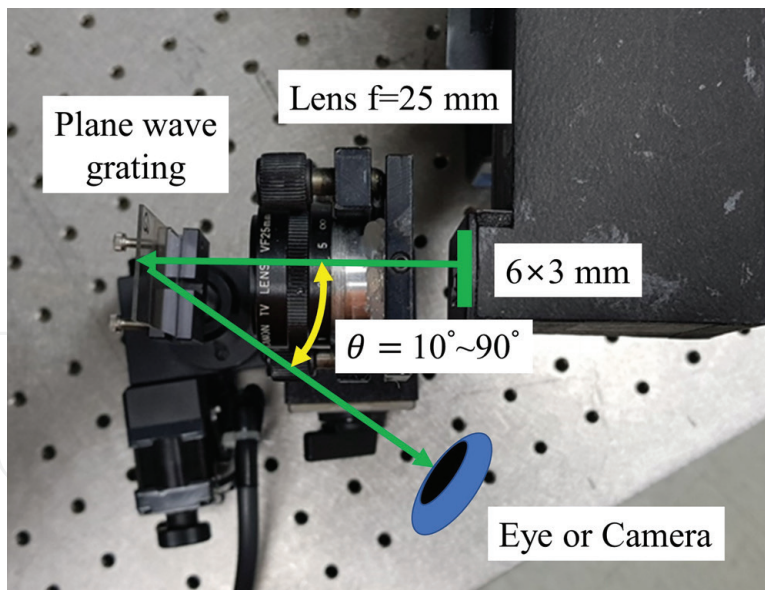


Figure 10.
Reconstruction system for monochromatic grating.

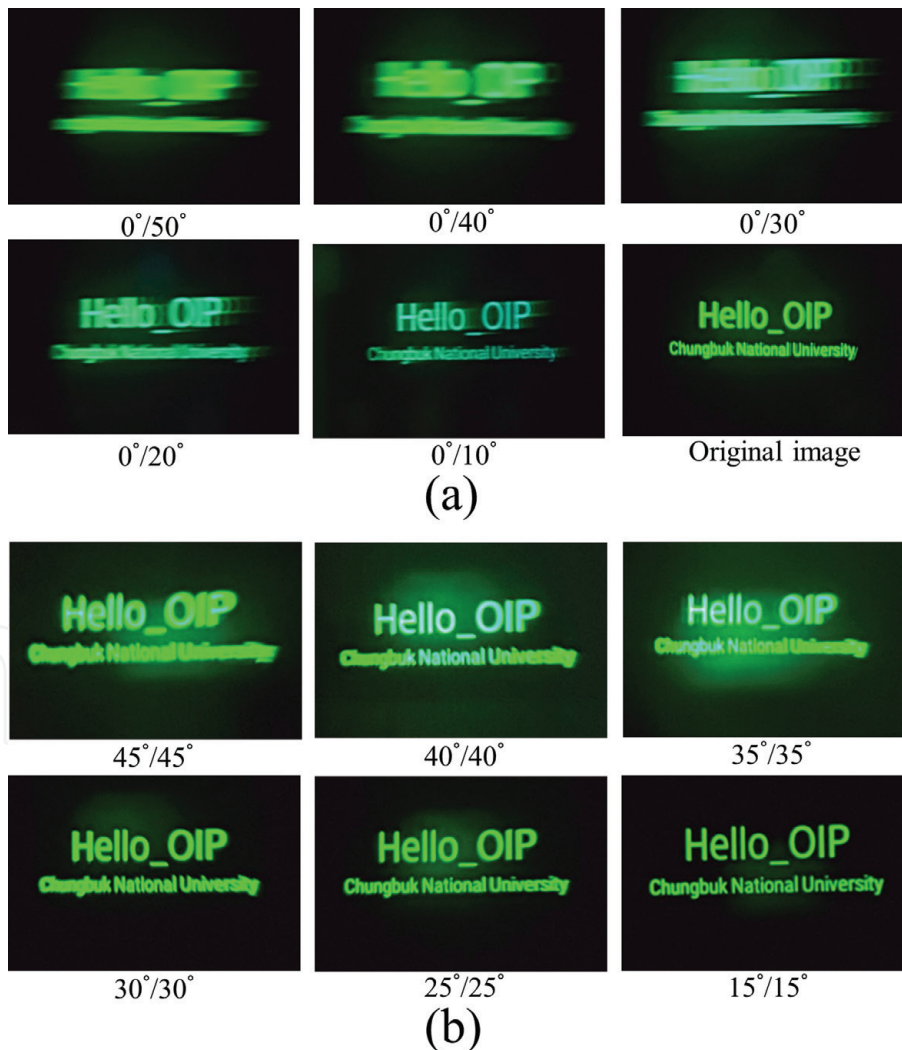


Figure 11.
Reconstruction images of monochromatic grating at (a) asymmetric recording angles (b) symmetric recording angles.

is similar to the wavelength selectivity bandwidth of the HOE, it can improve the brightness of the images displayed through the HOE. So, the spectral bandwidth of micro display can also play an important role in optimizing the full-color HOE.

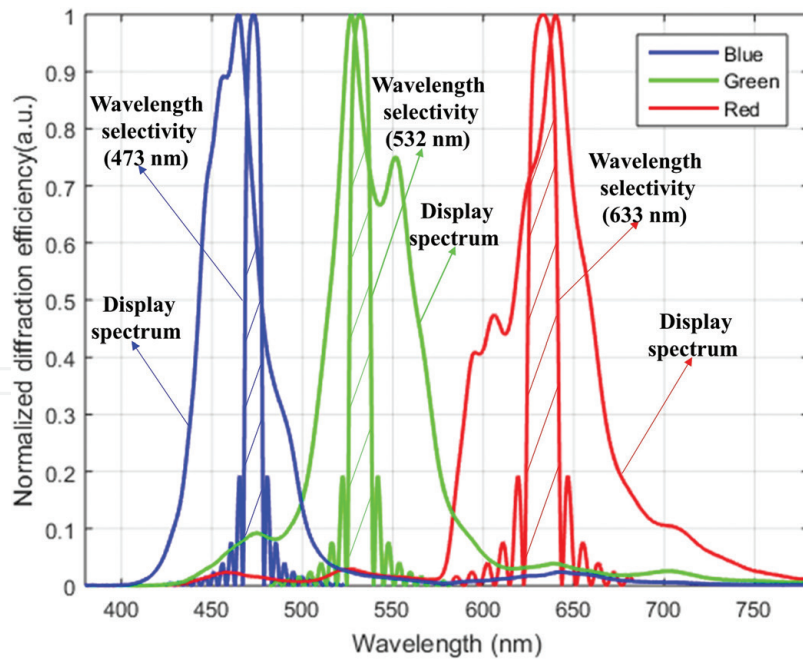


Figure 12.
 Micro display spectrum and wavelength selectivity of full-color HOE.



Figure 13.
 Diffraction image (left) and reflection image (right) of mixing color.

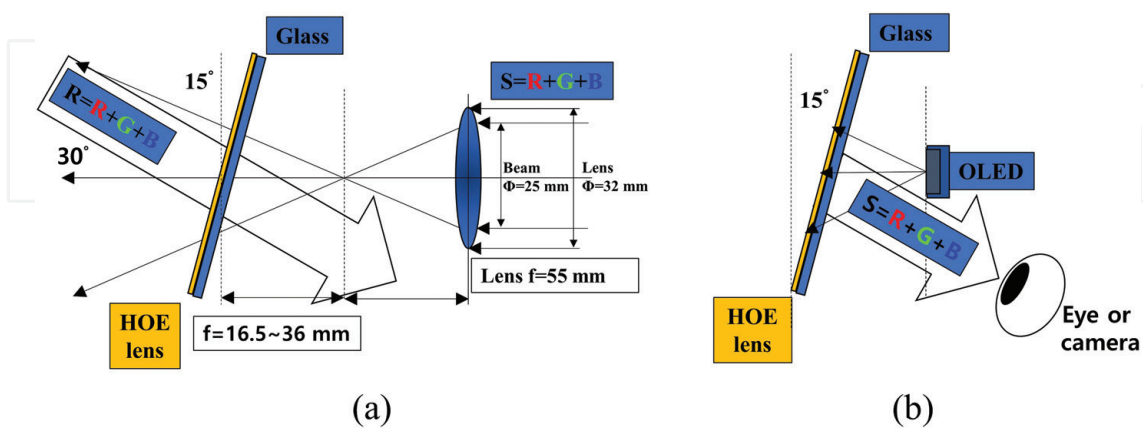


Figure 14.
 Symmetric ($\theta = 30^\circ$) recording of full-color HOE lens and reconstruction structure (a) recording, (b) reconstruction.

Figure 14 shows the optical configuration for recording full-color HOE lenses and reconstruction. If the focal length is recorded differently, the magnification will also depend on the focal length. In other words, the functions of the optical lens are recorded in the HOE and can be used as the HOE lens.

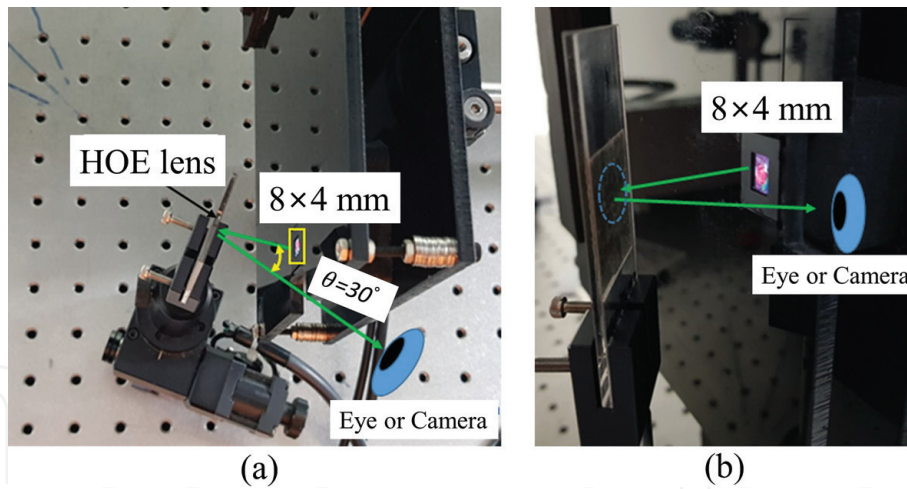


Figure 15. Reconstruction system using full-color HOE lens (a) top view, (b) side view.

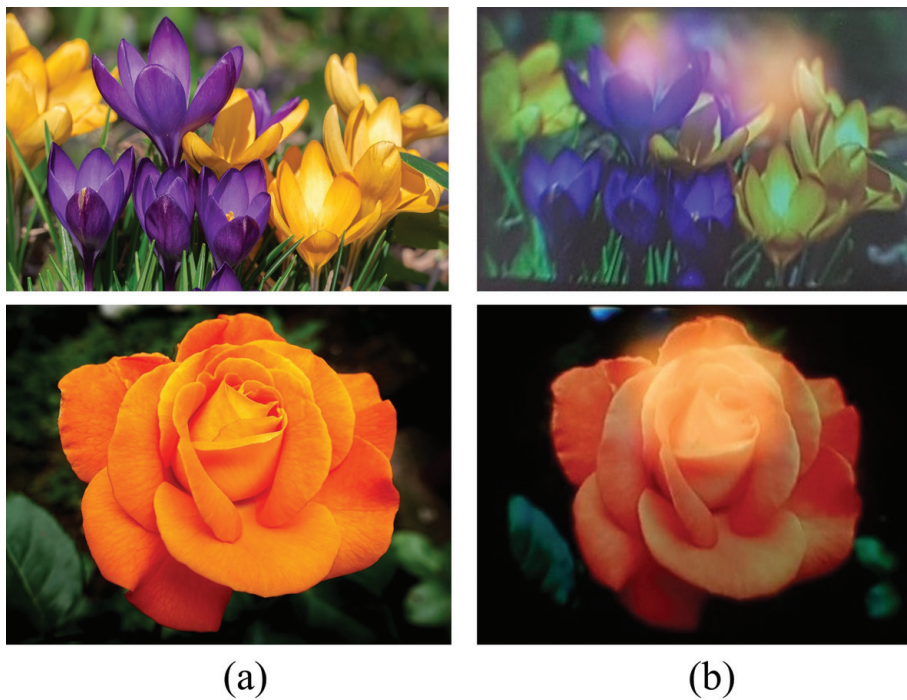


Figure 16. Full-color reconstruction image using full-color HOE lens (a) original image, (b) reconstruction image.

The optical lens used for recording the HOE lens was utilized with two optical lenses consisting of a focal length of 55 mm with less chromatic aberration and a full diameter of 32 mm. When recording HOE lenses, the characteristics of optical lenses such as chromatic aberrations and spherical aberrations are also recorded. So optical lenses with less distortion are used.

Figure 15 shows a reconstruction system that is configured to enlarge the reconstruction image with only the HOE lens. Because the distance between the display and the HOE lens is the focal length of the HOE lens, it is possible to see the enlarged image in the eye. The size of the full-color OLED micro display is 8 mm \times 4 mm, the number of the pixels is 1024 \times 768, the brightness is 300 cd/m².

Figure 16 shows full-color images reconstructed with HOE lens using OLED micro display. The system is configured so that OLED micro display is located at the focal length of the HOE lens and can be viewed by HUD method. The reconstruction images have good color uniformity and brightness performance. The blurred images shown at the upper of the reconstruction images are images

reflected by the substrate. Full-color OLED micro display can display the images by HUD method using HOE lens recorded by the optimum recording intensities for each wavelength.

4. Conclusions

The HOE is still developing in various fields such as a 3D display, holographic printer, HUD, HMD, AR and so on. Because of the lightweight, mass production advantages of the HOE, the conventional optical components are replacing with the HOE to simplify optical system. However, full-color HOE still has a limitation with color uniformity, low diffraction efficiency issues.

In this chapter, the shrinkage compensation method for the reflective diffraction grating was proposed to solve the Bragg angle shift problem. It can measure the maximum diffraction efficiency at the designed optical system without shifting the angle. And the optimum recording intensities for each wavelength were experimentally investigated by analyzing the non-response time of the recording materials. When the recording intensity was a red wavelength of 0.1 mW/cm^2 , a green wavelength of 0.11 mW/cm^2 , and a blue wavelength of 0.25 mW/cm^2 , respectively, the diffraction efficiency of the full-color HOE reached 56.84%. The fabricated full-color HOE lens can be used in HUD systems to display the images with good color uniformity.

Acknowledgements

This work was supported in part by the National Research Foundation of Korea (NRF) grant funded by the Korea government (NRF-2017R1A2B4012096), in part by the MSIT (Ministry of Science and ICT), Korea, under the ITRC (Information Technology Research Center) support program (IITP-2019-2015-0-00448) supervised by the IITP (Institute for Information & communications Technology Promotion).

IntechOpen

Author details

Hui-Ying Wu, Chang-Won Shin and Nam Kim*
School of Information and Communications Engineering,
Chungbuk National University, Cheongju, Chungbuk, South Korea

*Address all correspondence to: namkim@chungbuk.ac.kr

IntechOpen

© 2019 The Author(s). Licensee IntechOpen. This chapter is distributed under the terms of the Creative Commons Attribution License (<http://creativecommons.org/licenses/by/3.0>), which permits unrestricted use, distribution, and reproduction in any medium, provided the original work is properly cited. 

References

- [1] Hua H, Girardot A, Gao C, Rolland JP. Engineering of head-mounted projective displays. *Applied Optics*. 2000;**39**:3814-3824
- [2] Ando T, Matsumoto T, Takahashi H, Shimizu E. Head mounted display for mixed reality using holographic optical elements. *Memoirs of the Faculty of Engineering*. 1999;**40**:1-6
- [3] Mukawa H, Akutsu K, Matsumura I, Nakano S, Yoshida T, Kuwahara M, et al. A full-color eyewear display using planar waveguides with reflection volume holograms. *Journal of The Society For Information Display*. 2009;**17**:185-193
- [4] Yeom H-J, Kim H-J, Kim S-B, Zhang HJ, Li BN, Ji Y-M, et al. 3D holographic head mounted display using holographic optical elements with astigmatism aberration compensation. *Optics express*. 2015;**23**:32025-32034
- [5] Tomilin MG. Head-mounted displays. *Journal of Optical Technology*. 1999;**66**:528-533
- [6] Levola T, Aaltonen V. Near-to-eye display with diffractive exit pupil expander having chevron design. *Journal of the SID*. 2008;**16**:857-862
- [7] Levola T. Novel Diffractive Optical Components for Near-to-Eye Displays. *SID Symposium Digest of Technical Papers*. Vol. 372006. pp. 64-67
- [8] Oku T, Akutsu K, Kuwahara M, Yoshida T, Kato E, Aiki K, et al. High-luminance See-through Eyewear Display with Novel Volume Hologram Waveguide Technology. *SID Symposium Digest of Technical Papers*. 2015;**46**:192-195
- [9] Kasai I, Tanijiri Y, Endo T, Ueda H. A practical see-through head mounted display using a holographic optical element. *Optical Review*. 2000;**8**:241-244
- [10] Kim N, Piao Y-L, Wu H-Y. Holographic optical elements and application. In: Naydenova I, Nazarova D, Babeva T, editors. *Holographic Materials and Optical Systems*. Rijeka, Croatia: InTech; 2017. pp. 99-131. DOI: 10.5772/67297
- [11] Jang G, Lee C-K, Jeong J, Li G, Lee S, Yeom J, et al. Recent progress in see-through three-dimensional displays using holographic optical elements. *Applied Optics*. 2016;**55**:A71-A85
- [12] Hedili MK, Freeman MO, Urey H. Transmission characteristics of a bidirectional transparent screen based on reflective microlenses. *Optics Express*. 2013;**21**:24636-24646
- [13] Wakunami K, Hsieh P-Y, Oi R, Senoh T, Sasaki H, Ichihashi Y, et al. Projection-type see-through holographic three-dimensional display. *Nature Communications*. 2016;**7**:12954
- [14] Nakamura T, Yamaguchi M. Rapid calibration of a projection-type holographic light-field display using hierarchically upconverted binary sinusoidal patterns. *Applied Optics*. 2017;**56**:9520-9525
- [15] Kasezawa T, Horimai H, Tabuchi H, Shimura T. Holographic window for solar power generation. *Optical Review*. 2016;**23**:997-1003
- [16] Erdenebat M-U, Lim Y-T, Kwon K-C, Kim N. Waveguide-type head-mounted display system for AR application. In: Mohamudally N, editor. *State of the Art Virtual Reality and Augmented Reality Knowhow*. London, United Kingdom: InTech; 2018. pp. 41-58. DOI: 10.5772/intechopen.75172
- [17] Piao J-A, Li G, Piao M-L, Kim N. Full color holographic optical element fabrication for waveguide-type head mounted display using photopolymer.

Journal of the Optical Society of Korea.
2013;**17**:242-248

[18] Piao M-L, Kim N. Achieving high levels of color uniformity and optical efficiency for a wedge-shaped waveguide head-mounted display using a photopolymer. *Applied Optics*. 2014;**53**:2180-2186

[19] Kogelnik H. Coupled wave theory for thick hologram gratings. *Bell System Technical Journal*. 1969;**48**:2909-2947

[20] Shin C-W, Vu V-T, Kim N, An J-W, Suh D, Park Y, et al. Holographic polarization-selective module based on a small Dove prism coupler for magneto-optical pickup heads. *Applied Optics*. 2005;**44**:4248-4254

[21] Chen JH, Su DC, Su JC. Shrinkage- and refractive-index shift-corrected volume holograms for optical interconnects. *Applied Physics Letters*. 2002;**81**:1387-1389

[22] Shin C-W. Holographic Optical Elements for Full Color Augmented Reality Display [thesis]. Korea: Chungbuk National University; 2019